Journal of Neurochemistry
Lippincott-Raven Publishers, Philadelphia

Functional Characterization of Human *N*-Methyl-D-Aspartate Subtype 1A/2D Receptors

Stephen D. Hess, Lorrie P. Daggett, Charles Deal, Chin-Chun Lu, Edwin C. Johnson, and Gönül Veliçelebi

SIBIA Neurosciences, Inc., La Jolla, California, U.S.A.

Abstract: The human NMDAR2D subunit was cloned, and the pharmacological properties of receptors resulting from injection of transcripts encoding human NMDAR1A and NMDAR2D subunits in *Xenopus* oocytes were characterized by profiling NMDA receptor agonists and antagonists. We found that glutamate, NMDA, glycine, and D-serine were significantly more potent on hNMDAR1A/2D than on hNMDAR1A/2A or hNMDAR1A/2B. Also, the potencies of NMDA and glycine were higher for hNMDAR1A/2D than for hNMDAR1A/2C. Ifenprodil was more potent at hNMDAR1A/2B than at hNMDAR1A/2D, whereas 5,7-dichlorokynurenate was more potent at hNMDAR1A/2A than at hNMDAR1A/2D. As measured in transiently transfected human embryonic kidney 293 cells, the maximal inward current in the presence of external Mg^{2+} occurred at −40 mV, and full block was not observed at negative potentials. Kinetic measurements revealed that the higher affinity of hNMDAR1A/2D for both glutamate and glycine relative to hNMDAR1A/2A and hNMDA1A/2B can be explained by slower dissociation of each agonist from hNMDAR1A/2D. The hNMDAR1A/2D combination represents a pharmacologically and functionally distinct receptor subtype and may constitute a potentially important target for therapeutic agents active in the human CNS. **Key Words:** Clone—Oocyte—Voltage clamp—Patch clamp.
J. Neurochem. **70,** 1269–1279 (1998).

N-Methyl-D-aspartate (NMDA) receptors (NMDARs) are reportedly involved in learning and memory (Nakanishi, 1992) and several neuropathological states (Choi, 1988; Szatkowski and Attwell, 1994). To understand their role in these processes, NMDA receptor subunits have been cloned and studied extensively in recombinant expression systems. To date, cDNAs encoding eight splice variants of the NMDAR1 subunit and four NMDAR2 subunits (A–D) have been cloned from the rat and mouse (for review, see Hollmann and Heinemann, 1994; Mori and Mishina, 1995). Cloning of the human versions of these subunits has also been reported (Karp et al., 1993; Planells-Cases et al., 1993; Le Bourdellès et al., 1994; Foldes et al., 1994*a,b*; Adams et al., 1995; Hess et al., 1996). In situ hybridization studies in the rat have revealed that NMDAR1 transcripts are expressed throughout all regions of the CNS. In contrast, expression of the NMDAR2 transcripts is both developmentally and anatomically regulated. In adult rat brain, NMDAR2A is most prominent in the hippocampus and cerebellum, NMDAR2B is most highly expressed in the hippocampus, and NMDAR2C is almost exclusively localized to the cerebellum (Buller et al., 1994; Monyer et al., 1994).

The developmental and regional expression patterns of NMDAR2D mRNA in rat brain are different from those of NMDAR2A, 2B, or 2C (Monyer et al., 1994). Using in situ hybridization and immunoblot analyses in adult rat brain, Wenzel et al. (1995) determined that NMDAR2D immunoreactivity was most abundant in the thalamus, pallidum, subthalamic area, substantia nigra, superior colliculus, brainstem nuclei, and deep cerebellar nuclei. The distribution of NMDAR2D was nearly complementary to that of NMDAR2B, in that NMDAR2B immunoreactivity was strongest in the hippocampus, striatum, cerebral cortex, and olfactory bulb. Wenzel et al. (1996), using a histoblot technique in combination with RNase protection and immunoblot analyses, showed that of the two proposed splice variants, only NMDAR2D-2 is expressed in adult rat brain.

In addition to these differences in anatomical distribution, the functional properties of the NMDAR1A/2D combination are also different from those of the other NMDA subunit combinations. Most notable is that in human embryonic kidney (HEK) 293 cells expressing rat NMDAR1A/2D, the offset decay time constant of glutamate-induced inward currents is 5 s, which is 10–40-fold slower than that measured for NMDAR1A/2A, NMDAR1A/2B, or NMDAR1A/2C (Monyer et al., 1994). Also, the maximal inward cur-

Received July 28, 1997; revised manuscript received October 23, 1997; accepted October 24, 1997.

Address correspondence and reprint requests to Dr. S. D. Hess at SIBIA Neurosciences, Inc., 505 Coastal Boulevard South, Suite 300, La Jolla, CA 92037, U.S.A.

Abbreviations used: CGS 19755, *cis*-4-phosphonomethylpiperidine-2-carboxylic acid; DCKA, 5,7-dichlorokynurenic acid; HEK, human embryonic kidney; NMDA, *N*-methyl-D-aspartate; NMDAR, *N*-methyl-D-aspartate receptor; nt, nucleotide; SDS, sodium dodecyl sulfate.

rent recorded in the presence of 1 m*M* external Mg^{2+} occurs at −40 mV, compared with −25 mV determined for NMDAR1A/2A or NMDAR1A/2B. Moreover, at negative potentials NMDAR1A/2D is less sensitive to block by Mg^{2+} (Monyer et al., 1994). Recently, Momiyama et al. (1996) described low-conductance channels with a reduced sensitivity to block by extracellular Mg^{2+} in rat cerebellar Purkinje cells, spinal cord dorsal horn neurons, and deep cerebellar nuclear neurons, all of which express NMDAR2D mRNA. Their results suggest the NMDAR1A/2D combination makes up a functionally distinct subclass of native NMDARs. Behavioral analysis of the effects of ε4 (NMDAR2D) subunit knockout in mice revealed reduced spontaneous activity in an open field test and normal behavior in motor activity and anxiety tests (Ikeda et al., 1995).

The reported differences in the distribution and functional properties of NMDAR2D suggest that this subunit may play a distinct role in the CNS. Previous studies with recombinant rat (Buller et al., 1995; Williams, 1995; Buller and Monaghan, 1997) and mouse (Ikeda et al., 1992; Matsui et al., 1995; Williams, 1995) NMDARs have suggested that NMDAR1A/2D has a pharmacological profile distinct from those of other recombinant NMDA receptors. To this end, we cloned the human homologue of NMDAR2D, characterized the pharmacological properties of human NMDAR1A/2D complexes in *Xenopus* oocytes, and measured the biophysical characteristics of the recombinant receptor complex in HEK293 cells. We show that human NMDAR1A/2D (hNMDAR1A/2D) receptors display a pharmacological and biophysical profile distinct from those of other human recombinant NMDARs.

MATERIALS AND METHODS

cDNA libraries and construction of full-length NMDAR2D cDNA

To isolate cDNAs encoding hNMDAR2D, 10^6 recombinants from a human fetal brain λZAPII cDNA library (Stratagene) were screened with a 797-nucleotide (nt) cDNA fragment derived from a hNMDAR2A cDNA. The hybridization was performed using 30% formamide, 5× Denhardt's solution, 5× SSPE, 0.2% sodium dodecyl sulfate (SDS), and 200 mg/ml sonicated, denatured herring sperm DNA at 42°C, and the filters were washed with 2× SSPE and 0.2% SDS at 50°C. The hNMDAR2A probe was stripped from the filters by treatment with 0.2 *M* NaOH and 0.1% SDS at 37°C for 1 h. After the low-stringency screen, the filters were then rescreened using high-stringency hybridization conditions (as described above, except 50% formamide was used) with the hNMDAR2A probe described above, a 1,200 bp *Pst*I hNMDAR2B fragment, and a 950-bp *Acc*I hNMDAR2C fragment. The filters were washed with 0.1× SSPE and 0.2% SDS at 65°C. This secondary screen was used to eliminate the hNMDAR2A, hNMDAR2B, and hNMDAR2C cDNAs that were identified in the low-stringency screen. The 18 remaining faintly hybridizing plaques were further characterized by restriction mapping and DNA sequencing. One of the cDNAs isolated, NMDA96, was a partial cDNA with a 3′ sequence homologous to that of rat NMDAR2D-2 (Ishii et al., 1993). A 730-nt *Sma*I fragment from NMDA96 (nt 2,046–2,777) was then used to probe (hybridization conditions as above, except 50% formamide was used) 10^6 recombinants of a λZAP human fetal brain cDNA library specifically primed with an oligonucleotide based on the hNMDAR2D cDNA sequence. More than 200 hybridizing plaques were identified at a washing stringency of 0.1× SSPE and 0.1% SDS at 65°C, and 11 partial NMDAR2D cDNAs were characterized. Two overlapping hNMDAR2D cDNA clones, NMDA115 and NMDA96, were used to construct the full-length hNMDAR2D cDNA (Genbank accession no. U77783). The pBS-hNMDAR2D cDNA plasmid was constructed by ligating NMDA115 (nt −118 to 2,314) to NMDA96 (nt 2,315–4,205) through an *Spe*I site.

Reduction of the G–C content of hNMDAR2D

Monyer et al. (1994) have reported that the expression of rat NMDAR2D in *Xenopus* oocytes can be improved when the number of guanines (G) and cytosines (C) in the amino-terminal region is reduced. Therefore, we changed all the G–C dinucleotides in the first 150 nt of the hNMDAR2D sequence to A–T dinucleotides, which had no consequence on the deduced amino acid sequence. Using a modified version of the overlapping primer extension PCR protocol described by Ho et al. (1989) and the *pfu* DNA polymerase (Stratagene, La Jolla, CA, U.S.A.), four primers (SE362, SE363, SE364, and SE365) were placed in one reaction tube, and a 188-nt fragment of synthetic DNA was amplified. The reaction mixture (100 μl) contained 50 pmol each of SE362 and SE365 and 0.5 pmol each of SE363 and SE364. Nucleotides 1–26 of SE362 also introduce restriction sites for use in subcloning and a consensus ribosomal binding site (Kozak, 1986). The 188-nt PCR fragment was subcloned as a 160-nt *Kpn*I/*Not*I fragment into the pBS-hNMDAR2D construct to yield pBS-hNMDAR2D-GCMOD. A mammalian expression construct was prepared by digesting the pBS-hNMDAR2D-GCMOD cDNA with *Eco*RV/*Spe*I and subcloning into pCMV-T7-2. Recombinant hNMDAR2D and hNMDAR2D-GCMOD in vitro transcripts were synthesized from linearized plasmids using the mMessage mMachine T7 Promoter RNA Capping Kit (Ambion, Austin, TX, U.S.A.).

Electrophysiology

Stage V oocytes were isolated from *Xenopus laevis* using standard techniques (Goldin, 1992). Oocytes were typically injected with 50 nl containing 10–50 ng of one or more in vitro transcripts. At 2–6 days later, the cells were voltage-clamped (Warner Instruments OC-725B) with two microelectrodes and held at −80 mV in a bath containing 115 m*M* NaCl, 2.5 m*M* KCl, 1.8 m*M* $CaCl_2$, and 10 m*M* HEPES, pH 7.3. Unless otherwise mentioned, agonists were coapplied with 10 μ*M* glycine. Data collection and analysis were performed with Axotape and Clampfit software (Axon Instruments, Foster City, CA, U.S.A.).

The EC_{50} and IC_{50} values were estimated from curves fitted to the equation for a single-site sigmoidal dose–response curve with a variable slope: $Y = Y_{max}/(1 + (EC_{50}/X)^n)$, or $Y = Y_{max} - Y_{max}/(1 + (IC_{50}/X)^n)$, where n is the Hill coefficient and X is the concentration of the test compound. The concentration data are presented as the geometric mean with the lower and upper SD (or the arithmetic mean for Hill coefficients) for three to 11 oocytes. For the antagonists, the IC_{50} values were converted to K_b values

using the Leff–Dougall (Leff and Dougall, 1993) variant of the Cheng–Prusoff equation: $K_b = IC_{50}/[2 + ([A]/[A_{50}])^n]^{1/n} - 1$, where A is the agonist used and A_{50} is the EC_{50} value for the agonist. The geometric means for the concentration or K_b data, or arithmetic means for Hill coefficients, were tested for significant differences between receptor subtypes using either a two-tailed *t* test or ANOVA with post hoc Student–Newman–Keuls or Mann–Whitney Rank Sum tests. The post hoc tests (SigmaStat, ver. 1.01; Jandel Corp.) examined whether the means were different at $p < 0.05$ but did not calculate an absolute *p* value; therefore, the differences may be larger than stated in the text and tables.

HEK293 cells were transfected using the Ca^{2+} phosphate coprecipitation method described previously (Kingston, 1996). Forty-eight hours after transfection, currents were recorded using the whole-cell mode of the patch-clamp technique. Pipettes with resistances of 1.4–2.5 MΩ were used to record from cells plated on poly-L-lysine-coated coverslips that were continuously superfused with extracellular solution containing 135 m*M* NaCl, 5.0 m*M* KCl, 2.0 m*M* $CaCl_2$, 5.0 m*M* HEPES, and 11 m*M* glucose, pH 7.3. High-Na^+ Ringer's contained 160 m*M* NaCl and 5.0 m*M* HEPES, and high-Ca^{2+} Ringer's contained 110 m*M* $CaCl_2$ and 5.0 m*M* HEPES; the osmolality of these solutions was adjusted with mannitol. The pipette solution contained 135 m*M* $CsCl_2$, 10 m*M* EGTA, 10 m*M* HEPES, 1 m*M* $MgCl_2$, and 4 m*M* ATP, pH 7.4.

Cells were held at −60 mV, and currents were elicited by application of agonists via a pressure pipette positioned within 20–30 μm of the cell or by using a flow pipe array positioned by a piezoelectric element. The speed of solution exchange for the piezoelectric-controlled array was determined by changing the solution flowing over an open patch pipette from extracellular solution to 1:10 diluted extracellular solution. The time required for the resulting current to rise from 10 to 90% of the maximal value was ~500 μs. For analysis of current–voltage properties, cells were held at −60 mV and stepped to −100 mV for 2 ms, and subsequently the command potential was ramped from −100 to +100 mV in 1.8 s. Currents obtained in the absence of agonists were subtracted from those obtained in the presence of agonists to obtain the agonist-dependent current. To study the voltage dependence of block by external Mg^{2+}, leak and agonist-evoked current pairs in the absence of added external Mg^{2+} were first obtained, followed by application of the agonists in extracellular solution containing 1 m*M* external Mg^{2+}, and finally application of the agonists in nominally Mg^{2+}-free extracellular solution. The membrane potentials were not corrected for a junction potential of ~3 mV as measured with an open patch pipette on changing the bath solution from extracellular solution to a high (135 m*M*) Na^+ solution or a high (110 m*M*) Ca^{2+} solution.

Currents were filtered at 1 kHz and digitized at 2 kHz, and the experiments were performed and analyzed using pClamp software (Axon Instruments). All experiments were performed at room temperature (18–24°C).

For noise analysis, 1 m*M* NMDA/100 μ*M* glycine-induced currents were filtered at 1 kHz (eight-pole Butterworth) and sampled at 400-μs intervals. Power spectral analysis was performed as described previously (Varney et al., 1996).

Materials

NMDA, glycine, and D-serine were obtained from Sigma Chemical Co. (St. Louis, MO, U.S.A.). 5,7-Dichlorokynurenic acid (DCKA) and ifenprodil were from Research Biochemicals International (Natick, MA, U.S.A.). *cis*-4-Phosphonomethylpiperidine-2-carboxylic acid (CGS 19755) was obtained from the Pharma Division of Novartis (Basel, Switzerland).

RESULTS

Characterization of hNMDAR2D cDNA

A full-length hNMDAR2D cDNA, corresponding to the rat splice variant NMDAR2D-2 (Ishii et al., 1993), was constructed from overlapping cDNAs isolated from human fetal brain libraries. In brief, an hNMDAR2A cDNA fragment was used to isolate a partial hNMDAR2D cDNA from a human fetal brain cDNA library. This cDNA was subsequently used to screen a library made from cDNA synthesized with primers specific for hNMDAR2D, as described in Materials and Methods. Two overlapping clones were isolated and used to construct a full-length cDNA encoding hNMDAR2D.

The deduced amino acid sequences of hNMDAR2D and rat NMDAR2D-2 subunits (Ishii et al., 1993; Monyer et al., 1994) are compared in Fig. 1. The hNMDAR2D receptor contains 1,336 amino acids and thus is 13 residues longer than the rat homologue. The calculated molecular mass of the mature hNMDAR2D polypeptide is 144 kDa. The deduced amino acid sequences of hNMDAR2D and rat NMDAR2D cDNAs are 95.4% identical. Adopting the membrane topography proposed for rat GluR3 (Bennett and Dingledine, 1995) or rat NMDAR1 (Hirai et al., 1996), all six putative glycosylation sites and seven of the eight putative protein kinase C phosphorylation sites are conserved between the hNMDAR2D and rat NMDAR2D sequences. The hNMDAR2D sequence lacks one putative protein kinase C site identified in the rat ($Thr^{1,271}$), owing to the substitution of an alanine ($Ala^{1,284}$) at the homologous position.

Pharmacological characterization of human heteromeric NMDARs in *Xenopus* oocytes

Application of 10 μ*M* glutamate and 10 μ*M* glycine to oocytes injected with transcripts encoding hNMDAR1A and hNMDAR2D (n = 7 cells) elicited currents that were indistinguishable in magnitude from those in oocytes expressing hNMDAR1A alone. In contrast, oocytes from the same frog injected with transcripts encoding hNMDAR1A and hNMDAR2B gave currents that were substantially larger than those seen in oocytes expressing hNMDAR1A alone. Because Monyer et al. (1994) previously demonstrated that reducing the G–C dinucleotide content for the rat NMDAR2D cDNA improved heterologous expression of the NMDAR2D subunit, we exchanged all of the possible G or C nucleotides for A or T, respectively, in the human clone without altering the deduced amino acid sequence and thus reduced the G–C dinucleotide content from 87.6 to 58.7% between nucleotides 1 and 150 in the hNMDAR2D cDNA. Currents from one batch of oocytes (n = 5 cells) injected with transcripts encoding

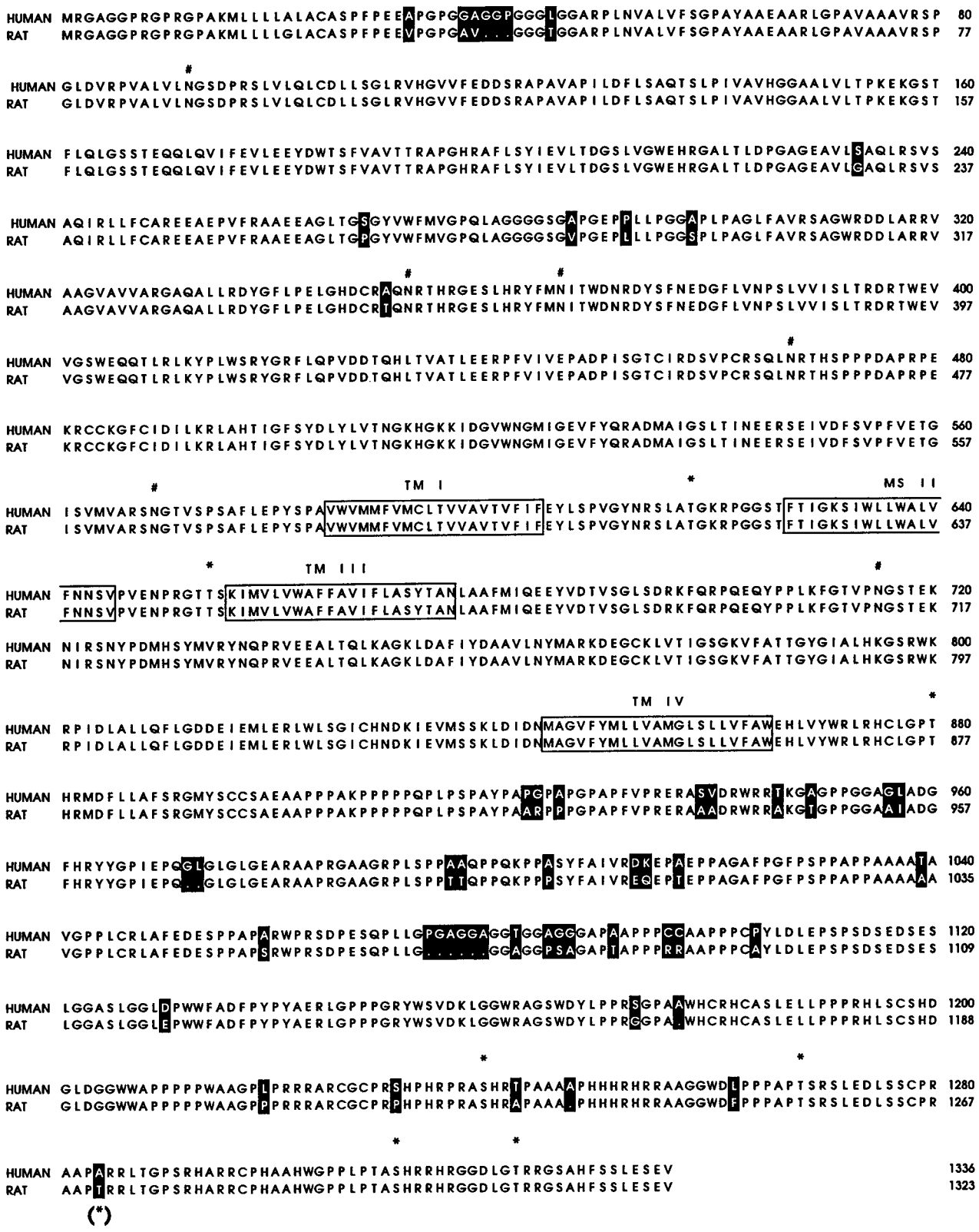

FIG. 1. Comparison of deduced amino acid sequences for hNMDAR2D and rat NMDAR2D subunits. The rat sequence is from Ishii et al. (1993). Shaded residues denote divergence between the different subunits. TMI, TMIII, and TMIV are the putative membrane spanning regions. MSII is either a membrane-spanning region (Wo and Oswald, 1994) or a reentrant membrane domain (Bennett and Dingledine, 1995). Consensus protein kinase C phosphorylation sequences are indicated (*), as are consensus glycosylation sequences (#).

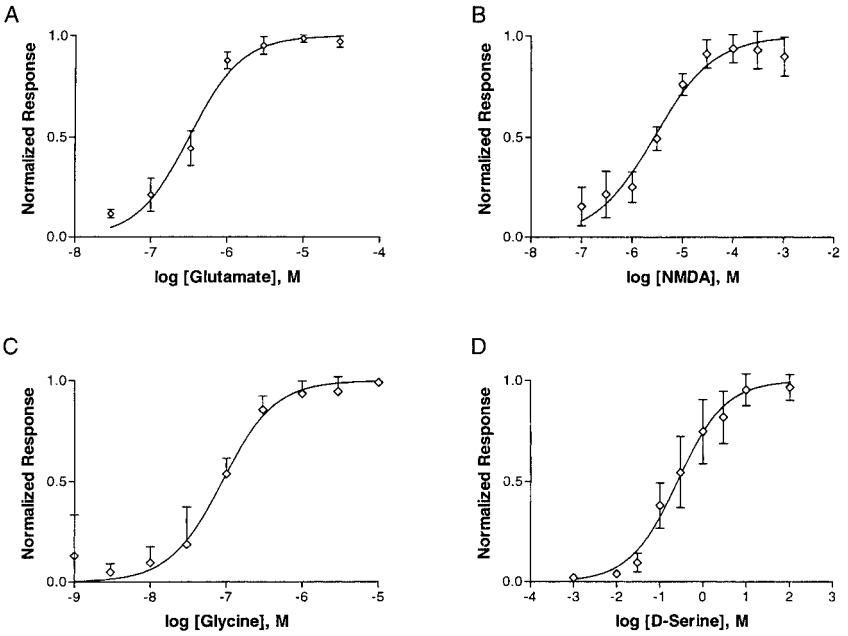

FIG. 2. Concentration–response curves for (**A**) glutamate, (**B**) NMDA, (**C**) glycine, and (**D**) serine for hNMDAR1A/2D expressed in *Xenopus* oocytes. Glutamate and NMDA sensitivities were determined in the presence of a saturating concentration of glycine. Glycine and D-serine sensitivities were determined in the presence of 100 μM NMDA. Data are mean ± SD (bars) normalized responses from four or five cells. The solid lines are fits to the equation $Y = Y_{max}/[1 + (EC_{50}/X)^n]$, with Y_{max} constrained to 1.0.

hNMDAR1A and G–C-reduced hNMDAR2D were significantly larger than those measured in oocytes injected with hNMDAR1A alone (415 ± 209 vs. 8.5 ± 7.1 nA; 15 and 25 cells, respectively; $p < 0.0001$ by t test). As described in Materials and Methods, the G–C-reduced hNMDAR2D cDNA was subcloned into suitable vectors for synthesis of in vitro transcripts as well as for expression in mammalian cells. The pharmacological and biophysical properties of the hNMDAR1A/2D receptors were examined in oocytes and HEK293 cells, respectively.

We examined the potencies of glutamate, NMDA, glycine, and D-serine to activate hNMDAR1A/2D receptors in oocytes (Fig. 2). From these studies, we determined the EC_{50} values and Hill coefficients listed in Table 1. The results indicated that the potencies of all four agonists were significantly higher for hNMDAR1A/2D than those we previously obtained for hNMDAR1A/2A and hNMDAR1A/2B also expressed in oocytes (Hess et al., 1996; all comparisons, $p < 0.05$ by ANOVA). Also, the potencies of NMDA and glycine were significantly higher for hNMDAR1A/2D than those for hNMDAR1A/2C (Deal et al., 1996). The EC_{50} value of 70 nM determined for glycine is similar to those previously reported by Buller et al. (1995) and Ikeda et al. (1992) for rat and mouse NMDAR1A/2D, respectively. For NMDA, our EC_{50} estimate of 2.5 μM is approximately fourfold lower than that reported by Buller et al. (1995) for rat NMDAR1A/2D. For D-serine, we determined an EC_{50} of 300 nM, compared with the value of 170 nM reported by Matsui et al. (1995) for mouse NMDAR1A/2D.

The efficacy of NMDA was compared with that of

TABLE 1. *Summary of EC_{50} values and Hill coefficients for glutamate, NMDA, glycine, and D-serine for human NMDAR expressed in* Xenopus *oocytes*

	Glutamate	NMDA	Glycine	D-Serine
hNMDAR1A/2D	0.3 (0.2, 0.4)	2.5 (1.7, 3.6)	0.07 (0.06, 0.10)	0.3 (0.1, 0.7)
n_H	1.4 ± 0.3	0.8 ± 0.3	1.3 ± 0.7	0.9 ± 0.1
hNMDAR1A/2A	1.6 (0.6, 4.2)[a]	23.9 (13.2, 43.1)[a]	1.9 (1.7, 2.2)[a]	2.2 (1.5, 3.2)[a]
n_H	1.2 ± 0.1	1.1 ± 0.1	1.1 ± 0.2	1.0 ± 0.1
hNMDAR1A/2B	1.4 (0.7, 2.7)[a]	9.9 (7.8, 12.5)[a]	0.2 (0.1, 0.3)[a]	0.6 (0.2, 2.1)[a]
n_H	1.3 ± 0.4	1.1 ± 0.1	0.9 ± 0.3	0.8 ± 0.2
hNMDAR1A/2C		21.9 (16.6, 28.9)[a]	0.6 (0.4, 0.9)[a]	
n_H		0.9 ± 0.3	0.6 ± 0.2	

Data are geometric means (lower and upper SD), in μM, obtained from four to seven oocytes. The Hill coefficient (n_H) is given as arithmetic mean ± SD. Data for hNMDAR1A/2A and hNMDAR1A/2B are from Hess et al. (1996), and those for hNMDAR1A/2C are from Deal et al. (1996).

[a] $p < 0.05$ by ANOVA with post hoc Student–Newman–Keuls test, significantly different from the mean for hNMDAR1A/2D.

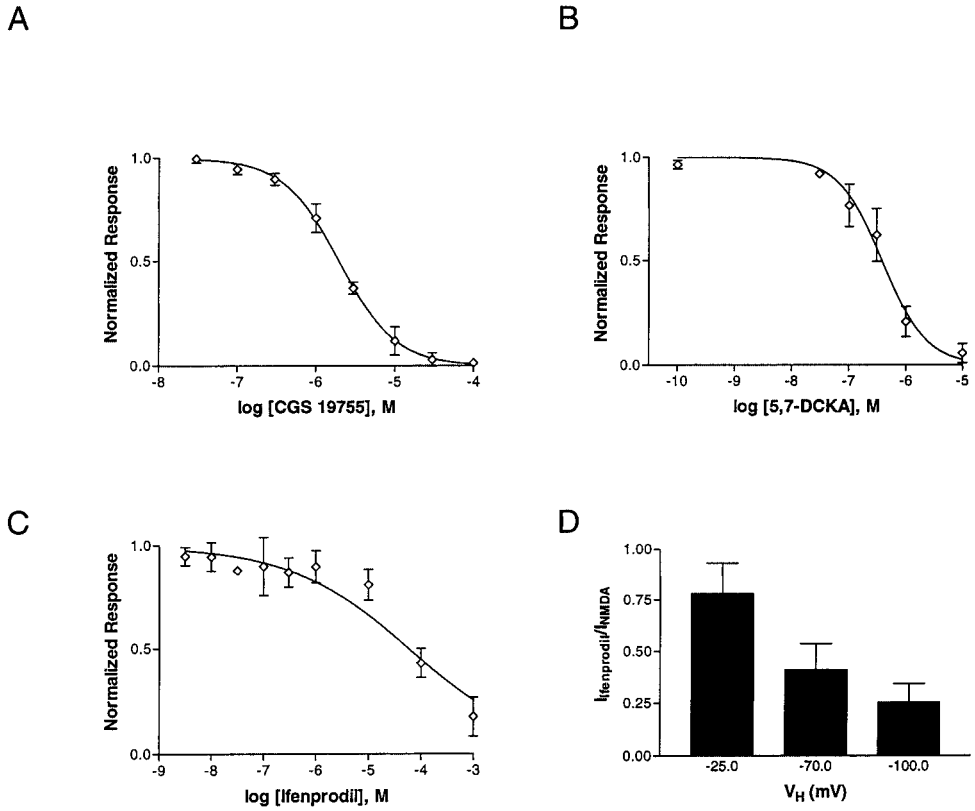

FIG. 3. Inhibition curves for (**A**) CGS 19755, (**B**) 5,7-DCKA, and (**C**) ifenprodil for hNMDAR1A/2D expressed in *Xenopus* oocytes. CGS 19755 was tested in the presence of 100 μM NMDA and 10 μM glycine, 5,7-DCKA was tested with 100 μM NMDA and 0.3 μM glycine, and ifenprodil was tested with 300 μM NMDA and 30 μM glycine. Data are mean ± SD (bars) normalized responses from four or five cells. The solid lines are fits to the equation $Y = Y_{max} - Y_{max}/[1 + (IC_{50}/X)^n]$, with Y_{max} constrained to 1.0. **D:** Voltage-dependent inhibition of hNMDAR1A/2D by 100 μM ifenprodil. Data represent the normalized steady-state current [mean ± SD (bars) values from five or six cells] at the indicated holding potential. The inhibition observed at −70 and −100 mV was significantly different from that observed at −25 mV ($p < 0.05$ by ANOVA with repeated measures and post hoc Student–Newman–Keuls test), whereas there was no significant difference for the inhibition observed at −70 versus −100 mV.

glutamate in eight oocytes by measuring the mean current amplitude in each cell elicited by three applications of 300 μM NMDA and 10 μM glycine and three applications of 30 μM glutamate and 10 μM glycine. The mean ± SEM ratio of the current amplitude elicited by NMDA to that elicited by glutamate was 1.003 ± 0.024 (n = 8), suggesting that NMDA is a full agonist, relative to glutamate, for hNMDAR1A/2D expressed in oocytes. Using electrophysiological recordings from stably transfected mammalian cells, Priestley et al. (1995) found that NMDA was 83 and 65% as efficacious as glutamate at hNMDAR1A/2A and hNMDAR1A/2B, respectively, and Varney et al. (1996) concluded using a fluorescent dye-based intracellular free Ca^{2+} concentration assay that NMDA was 70 and 74% as efficacious as glutamate at hNMDAR1A/2A and hNMDAR1A/2B, respectively. Further experiments are necessary to examine whether NMDA is a full agonist at NMDAR1A/2D, particularly when expressed in mammalian cells.

From concentration–response curves for the antagonists CGS 19755 (Fig. 3A), 5,7-DCKA (Fig. 3B), and ifenprodil (Fig. 3C), we determined the IC_{50} values for inhibition of hNMDAR1A/2D and calculated K_b values using the Leff–Dougall variant of the Cheng–Prusoff equation, thus adjusting the IC_{50} values relative to the concentration and the Hill coefficient of the agonist used. The antagonist results also indicated a unique pharmacology for hNMDAR1A/2D relative to hNMDAR1A/2A, hNMDAR1A/2B, or hNMDAR1A/2C (Table 2). The K_b estimate for 5,7-DCKA showed that this glycine site antagonist was threefold less potent at hNMDAR1A/2D than at hNMDAR1A/2A and is twofold more potent at hNMDAR1A/2D than at hNMDAR1A/2C but did not have a significantly different potency at hNMDAR1A/2D versus hNMDAR1A/2B. Furthermore, the noncompetitive antagonist ifenprodil was significantly more potent at hNMDAR1A/2B than at hNMDAR1A/2A, hNMDAR1A/2C, and hNMDAR1A/2D, whereas this compound did not distinguish between hNMDAR1A/2D and hNMDAR1A/2C, hNMDAR1A/2D and hNMDAR1A/2A, or hNMDAR1A/2A and hNMDAR1A/2C. CGS 19755 displayed no subtype

TABLE 2. *Summary of Leff–Dougall K_b or IC_{50} values and Hill coefficients for antagonists*

	CGS 19755	5,7-DCKA	Ifenprodil
hNMDAR1A/2D	0.30 (0.27, 0.34)	0.09 (0.06, 0.13)	75.9 (56.2, 102.3)
n_H	1.3 ± 0.2	1.3 ± 0.4	0.6 ± 0.3
hNMDAR1A/2A	0.36 (0.30, 0.44)	0.03 (0.02, 0.05)[a]	39.5 (17.5, 89.5)
n_H	1.1 ± 0.1	0.7 ± 0.1	0.6 ± 0.1
hNMDAR1A/2B	0.37 (0.26, 0.51)	0.05 (0.03, 0.09)	0.114 (0.04, 0.31)[a]
n_H	1.1 ± 0.2	1.2 ± 0.5	0.8 ± 0.2
hNMDAR1A/2C	0.27 (0.18, 0.40)	0.17 (0.11, 0.26)[a]	29.1 (6.6, 128.1)
n_H	1.2 ± 0.1	0.9 ± 0.2	0.6 ± 0.1

Data are geometric means (lower and upper SD), in μM, for the K_b for CGS 19755 and 5,7-DCKA or the IC_{50} for ifenprodil obtained from three to five oocytes. The Hill coefficient (n_H) is given as mean ± SD. Data for hNMDAR1A/2A and hNMDAR1A/2B are from Hess et al. (1996), and those for hNMDAR1A/2C are from Deal et al. (1996) and C. Deal et al. (unpublished data).

[a] $p < 0.05$ by ANOVA with post hoc Student–Newman–Keuls test, significantly different from the mean for hNMDAR1A/2D.

selectivity against the four subunit combinations tested.

Williams (1993) reported that rat NR1A/NR2A receptors expressed in oocytes were inhibited by ifenprodil in a voltage-dependent fashion. We therefore examined whether the low-affinity block of hNMDAR1A/2D receptors was voltage-dependent. The inhibition observed with 100 μM ifenprodil was significantly greater at a holding potential of −100 or −70 mV than that observed at −25 mV (Fig. 3D), which is consistent with a voltage-dependent mechanism of channel block.

These results show that hNMDAR1A/2D has a high sensitivity to NMDA, glycine, and D-serine and therefore has an agonist profile more closely resembling that of hNMDAR1A/2B than that of hNMDAR1A/2A or hNMDAR1A/2C. As for its antagonist profile, hNMDAR1A/2D is indistinguishable from the other three combinations in terms of sensitivity to block by CGS 19755 at the glutamate site, is equivalent to hNMDAR1A/2B in terms of sensitivity to block by 5,7-DCKA at the glycine site, and resembles hNMDAR1A/2A and NMDAR1A/2C in terms of sensitivity to block by ifenprodil at a noncompetitive site or sites. Thus, compared with hNMDAR1A/2A, hNMDAR1A/2B, and hNMDAR1A/2C, the hNMDAR1A/2D receptors display a unique pharmacological profile.

Biophysical properties of hNMDAR1A/2D

We transiently transfected HEK293 cells with plasmids encoding hNMDAR1A and hNMDAR2D and examined the biophysical properties of the recombinant receptors. Figure 4A shows the current–voltage relationship obtained by ramping the membrane potential from −100 to +100 mV in the presence of 1 mM NMDA/100 μM glycine in extracellular solution without added Mg^{2+} or in extracellular solution containing 1.0 mM Mg^{2+}. In the Mg^{2+}-containing solution, the maximal inward current occurred at −38.4 ± 4.1 mV (mean ± SD, n = 4 cells). Monyer et al. (1994) reported a value of −45 mV for rat NMDAR1A/2D expressed in HEK293 cells. Similar to the observations by Monyer et al. (1994), we did not observe full block even at −100 mV.

Power spectra were derived from analysis of the inward current (V_H = −60 mV) elicited by 1 mM NMDA/100 μM glycine in nominally Mg^{2+}-free conditions. A representative spectrum for one cell is shown in Fig. 4B, where the solid line shows the fit of the data to a single Lorentzian function. Because the data were fit well by a single Lorentzian function, there is likely only one major kinetic event underlying the NMDA-induced current. From four cells, estimates of the corner frequency (169.25 ± 42.72 Hz, n = 4), mean open time (1.0 ± 0.3 ms), and single channel conductance (24.5 ± 4.7 pS) were obtained. These estimates are similar to the mean open times of 1.01 and 1.28 ms for the 35 and 17 pS events obtained by Wyllie et al. (1996) with single-channel recordings in oocytes expressing rat NMDAR1A/2D.

We examined the association and dissociation rates of glutamate and glycine. Previously, it was shown that the time constant for current decay following removal of glutamate is 10–40-fold slower for rat NMDAR1A/2D than for NMDAR1A/2A, NMDAR1A/2B, or NMDAR1A/2C (Monyer et al., 1994). To measure the relative contributions of glutamate and glycine to the slow decay, we measured the current decay for hNMDAR1A/2D following the removal of glutamate in the continued presence of glycine or following the removal of glycine in the continued presence of glutamate. A piezoelectric-controlled fast solution exchange system was used to apply and remove agonists, and inward currents were recorded from cells held at −60 mV. Following an 800-ms application of 100 μM glutamate/10 μM glycine, the removal of glutamate resulted in relaxation of the current (Fig. 4C) that was best fit by a single-exponential

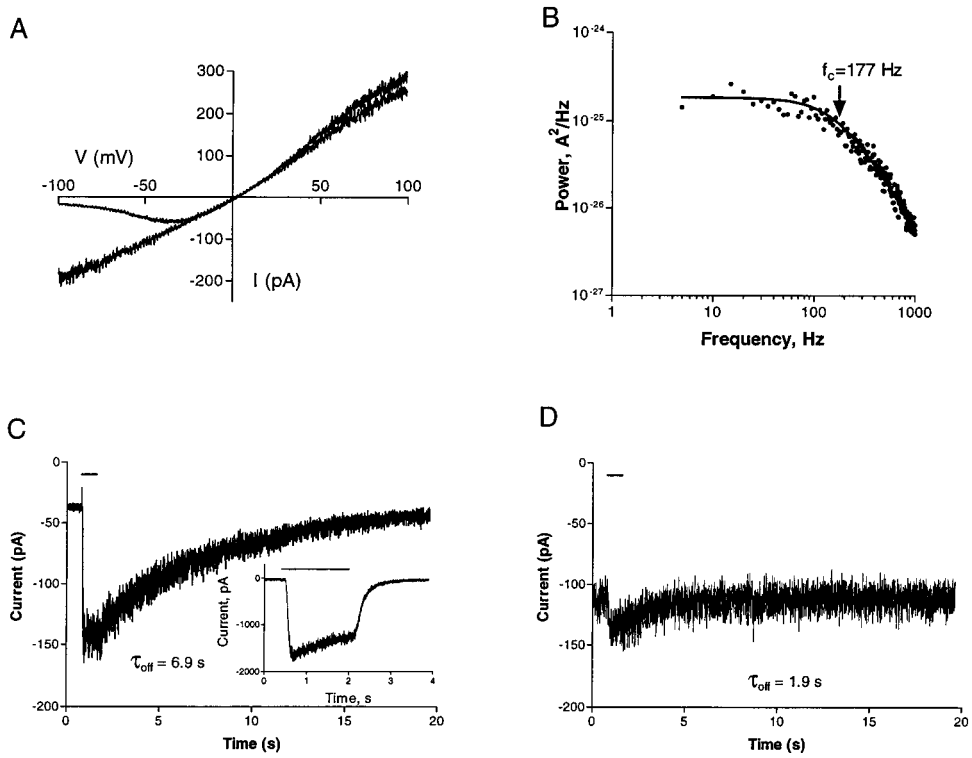

FIG. 4. Whole-cell currents recorded from hNMDAR1A/2D expressed in HEK293 cells. **A:** Leak-corrected current–voltage relationships obtained in the presence or absence of 1 m*M* Mg^{2+} Ringer's solution by changing the membrane potential from −100 to 100 mV in the presence of 1 m*M* NMDA and 100 μM glycine. **B:** Power spectrum derived from analysis of the inward current (V_H = −60 mV) elicited by 1 m*M* NMDA/100 μM glycine in nominally Mg^{2+}-free conditions. The solid line shows the fit of the data to a single Lorentzian function, and the corner frequency (f_c) is indicated by the arrow. **C** and **D:** Current responses to an 800-ms application of 100 μM glutamate during continuous application of 10 μM glycine (C) or application of 10 μM glycine during continuous application of 100 μM glutamate (D). The **inset** in C shows the response of an HEK cell stably expressing hNMDAR1A/2A to a 1.6-s application of 100 μM glutamate during continuous application of 10 μM glycine.

decay. From five cells, τ_{off} for glutamate was 6.3 ± 0.4 s (mean ± SD), compared with the value of 4.8 s reported for rat NMDAR1A/2D by Monyer et al. (1994). For comparison, Fig. 4C, inset, shows the 29-fold faster relaxation of the current (τ_{off} = 216 ms) from an HEK293 cell stably expressing hNMDAR1A/2A receptors. Following removal of glycine, the current decayed with a τ_{off} of 1.8 ± 0.2 s (n = 6 cells; Fig. 4D).

From the concentration–response data shown in Fig. 2, we used a two-equivalent binding site model (Patneau and Mayer, 1990) to estimate microscopic K_D values (geometric mean, lower and upper SD) of 108 (73, 159) and 39 (13, 114) n*M* for glutamate and glycine, respectively (n = 5 cells each). We estimated k_{on} values of 1.47 and 14 μM^{-1} s^{-1} for glutamate and glycine by dividing the respective k_{off} ($1/\tau_{off}$) values by the respective microscopic K_D values. These values are similar to the values of 4.9 and 8.3 μM^{-1} s^{-1} reported for glutamate and glycine, respectively, by Clements and Westbrook (1991) from measurements of association kinetics from outside-out patches from cultured hippocampal neurons. The overall agreement between our k_{on} estimates derived from the concentration-response curves for hNMDAR1A/2D and the k_{on} estimates from kinetic data obtained from hippocampal neurons suggests that the actual microscopic on-rates for hNMDAR1A/2D receptors may be reasonably close to those estimated for native NMDA receptors in cultured hippocampal neurons. We also determined that for hNMDAR1A/2D the currents activated by 100 μM glutamate or 10 μM glycine increased from 10 to 90% of the maximal value within 30.3 ± 14.0 (mean ± SD, n = 10 cells) and 40.7 ± 14.0 ms (n = 3 cells), respectively. These values are also similar to the values of 10 ms for 200 μM glutamate and 62 ms for 5 μM glycine determined for native receptors in hippocampal neurons by Clements and Westbrook (1991). Taken together, the kinetic data we obtained for glutamate and glycine suggest that, as measured using recombinant receptors expressed in oocytes, the higher affinity of hNMDAR1A/2D for both agonists, relative to hNMDAR1A/2A and hNMDAR1A/2B, is largely explained by the much slower dissociation rates of each agonist from hNMDAR1A/2D.

Subunit-specific differences in the Ca^{2+} permeability of NMDA receptors could play important roles in both normal and disease states. We estimated the Ca^{2+}

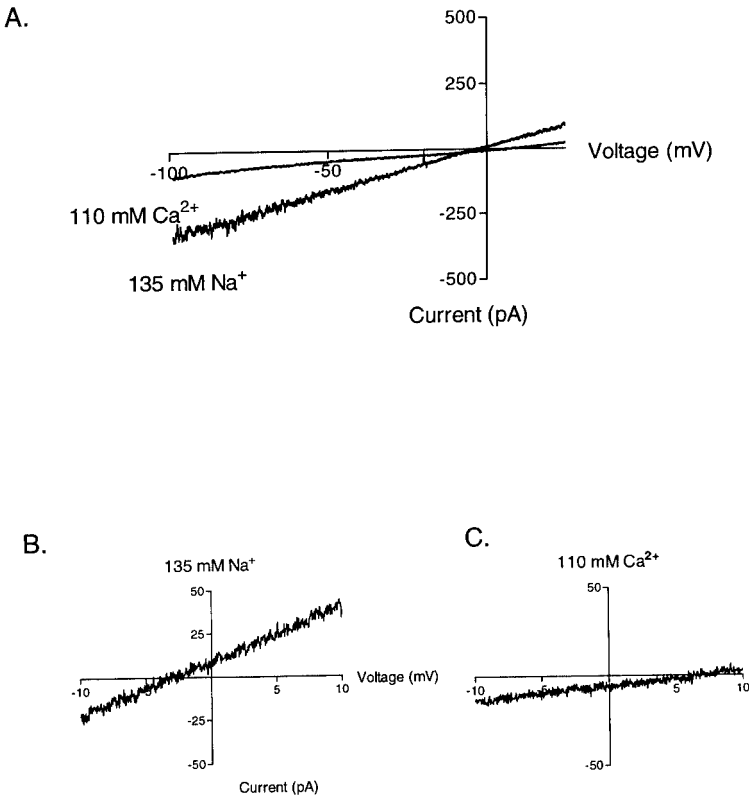

FIG. 5. Calcium permeability of hNMDAR1A/2D. **A:** Leak-corrected recordings of the current elicited by 1 m*M* NMDA and 100 μM glycine while ramping the membrane potential from −100 to +40 mV with 110 m*M* Ca^{2+} or 135 m*M* Na^+ as the external charge carrier are shown. **B** and **C:** The voltage axis is expanded for each of the two charge carriers to show the reversal potential of the current more clearly.

permeability of the hNMDAR1A/2D receptor by examining the shift in the reversal potential of the NMDA current in external solutions containing either Na^+ or Ca^{2+} as the sole charge carrier. In four cells, the reversal potential of the current induced by NMDA and glycine was −3.5 ± 3.9 mV when recorded in extracellular solution without added Mg^{2+}. The reversal potential shifted to −8.9 ± 5.7 mV in 135 m*M* Na^+ and to 9.2 ± 3.3 mV in 110 m*M* Ca^{2+} (Fig. 5A; expanded scale in B and C). The 18.1 mV difference in reversal potentials indicates a substantial Ca^{2+} permeability for hNMDAR1A/2D. Monyer et al. (1994) reported a similar shift of 20.9 mV for rat NMDAR1A/2D expressed in HEK293 cells.

DISCUSSION

We have isolated the cDNA encoding the NMDAR2D subunit and functionally coexpressed it with hNMDAR1A. Overall, the deduced amino acid homology between the hNMDAR2D and rat NMDAR2D cDNAs is 95.4%. However, the deduced amino acid sequence homology is reduced to 83.5% in the carboxyl-terminal region between Pro^{923} and $Ala^{1,243}$, where hNMDAR2D contains 10 more amino acids than the corresponding region in the rat homologue. It is interesting that, in hNMDAR2C, the amino acid sequence homology also diverges from the rodent sequence in the Gly^{925} to $Val^{1,326}$ region (Daggett et al., 1994). The differences in the amino acid sequences in this region of the hNMDAR2C and rat NMDAR2C subunits result from the divergence of the genomic sequences and not from alternative splicing (Daggett et al., 1994). Further experiments are necessary to address the basis of the divergence in the NMDAR2D sequences.

Recombinant hNMDAR1A/2D displays higher sensitivity for glutamate, NMDA, glycine, and D-serine compared with hNMDAR1A/2A and hNMDAR1A/2B (Hess et al., 1996) and has a higher affinity for NMDA and glycine than hNMDAR1A/2C (Deal et al., 1996). In summary, hNMDAR1A/2D receptors more closely resemble hNMDAR1A/2B receptors in their high sensitivity to NMDA, glycine, and D-serine but more closely resemble hNMDAR1A/2A and hNMDAR1A/2C receptors in their low sensitivity to ifenprodil and thus represent a pharmacologically distinct subtype. Previously, Williams (1995) showed that rat NR1A/mouse ε4 receptors expressed in oocytes were insensitive to spermine, histamine, and ifenprodil and therefore more closely resembled NMDAR1A/2C receptors. Buller and Monaghan (1997) showed that among binary rat NMDARs expressed in oocytes, the NMDAR1A/2D profile was characterized by a high affinity for NMDA and the antagonists (±) - 4 - (4 - phenylbenzoyl)piperazine - 2, 3 - dicarboxylic acid and α - amino - 5 - (phosphono - methyl)[1,1′-biphenyl]-3-propionic acid and low af-

finity for homoquinolinate and the antagonists D-(−)-2-amino-5-phosphonopentanoic acid, (*R,E*)-4-(3-phosphonoprop-2-enyl)piperazine-2-carboxylic acid, and (±)-6-(1*H*-tetrazol-5-ylmethyl)decahydroisoquinoline-3-carboxylic acid (LY233536).

We observed that the potency of glycine varies 27-fold across the four subunit combinations studied, whereas the potency of glutamate varies fivefold across the three combinations. Recent studies suggest that the residues important for glycine binding reside in the NMDAR1 subunit (Hirai et al., 1996) and those for glutamate reside in the NMDAR2 subunits (Laube et al., 1997). More detailed information on the protein–protein interactions between NMDAR subunits is required to understand the molecular determinants of agonist affinity or efficacy.

In addition to the pharmacological differences between hNMDAR1A/2D and the other binary combinations, these receptors have a unique biophysical profile. Most notable is that decay time constants of 6.3 and 1.8 s for glutamate and glycine are 28- and ninefold slower, respectively, than 226 and 195 ms defined for hNMDAR1A/2A receptors stably expressed in HEK293 cells. NMDAR1A/2D receptors are less sensitive to block by external Mg^{2+} than are NMDAR1A/2A or NMDAR1A/2B. Specifically, the maximal inward current for NMDAR1A/2D receptors recorded in the presence of 1 m*M* external Mg^{2+} occurs at approximately −40 mV, which is significantly more negative than the value of −25 mV reported for rat (Monyer et al., 1994) or human (Varney et al., 1996) NMDAR1A/2A or NMDAR1A/2B receptors. This suggests that, in response to glutamate release from presynaptic terminals, NMDAR1A/2D channels can open without the need for the concomitant activity of α-amino-3-hydroxy-5-methylisoxazole-4-propionate (AMPA) receptors. Thus, NMDAR1A/2D receptors may play a minor role as coincidence detectors compared with the other NMDA receptors. However, the unique kinetic properties we described for hNMDAR1A/2D receptors suggest that they could play an important role in temporal summation of events separated by as much as several seconds.

Intrathecal injection of NMDA produces persistent pain behavior in rats that is blocked by prior injection of the NMDA antagonist 2-amino-5-phosphonopentanoic acid and reduced by injection of substance P receptor antagonists (Liu et al., 1997). A similar reduction in pain behavior was also seen in neonates treated with capsaicin to destroy NMDAR-enriched C fibers, suggesting that the pain produced by NMDA is generated by the release of substance P from primary afferent nociceptors. These results, together with previous immunocytochemical data localizing NMDAR1 receptors near active zones in the presynaptic terminals of glutamatergic afferents in the spinal cord (Liu et al., 1994), led Liu et al. (1997) to suggest that NMDA acts at presynaptic receptors to facilitate and prolong the transmission of nociceptive messages, although they also noted that NMDA effects at postsynaptic receptors are possible. Results of in situ hybridization studies in rat spinal cord indicate that the mRNA for NMDAR2D is widely distributed, whereas that for NMDAR2C is confined to the substantia gelatinosa, and those for NMDAR2A and NMDAR2B are not detectable (Tölle et al., 1993). Although morphological data specifically colocalizing NMDAR1 and NMDAR2D or NMDAR2C subunits in pain pathways are not yet available, NMDAR1A/2D receptors may be important therapeutic targets for treatment of hyperalgesia, allodynia, and persistent pain following injury to tissue and nerves.

Because of their specific distribution in the brain and spinal cord, high sensitivity to agonists, reduced sensitivity to block by external Mg^{2+}, relief of block at less depolarized potentials, and the prolonged response to the application of agonist, NMDAR1A/2D receptors could integrate synaptic activity in a fashion quite different from the other NMDARs. These properties could, in concert with substantial permeability to Ca^{2+}, render the sustained release of glutamate during ischemia, stroke, or head trauma especially toxic to neurons that express NMDAR2D subunits. Also, inhibition of pre- and postsynaptic receptors containing NMDAR2D subunits could serve to lessen or alleviate several types of pain. Further experiments should address the role of NMDAR1A/2D receptors in both normal and pathologic physiology.

Acknowledgment: We wish to thank Novartis Pharma Research for providing CGS 19755, Steven Ellis for advice on cloning, and K. Lariosa, F.-F. Lin, and M. Urcan for technical assistance. We also thank Drs. M. Harpold, S. Madigan, and M. Varney for critically reading the manuscript and K. Payne for secretarial assistance.

REFERENCES

Adams S.-L., Foldes R. L., and Kamboj R. K. (1995) Human *N*-methyl-D-aspartate receptor modulatory subunit hNR3: cloning and sequencing of the cDNA and primary structure of the protein. *Biochim. Biophys. Acta* **1260,** 105–108.

Bennett J. A. and Dingledine R. (1995) Topology profile for a glutamate receptor: three transmembrane domains and a channel-lining reentrant membrane loop. *Neuron* **14,** 373–384.

Buller A. L. and Monaghan D. T. (1997) Pharmacological heterogeneity of NMDA receptors: characterization of NR1a/NR2D heteromers expressed in *Xenopus* oocytes. *Eur. J. Pharmacol.* **320,** 87–94.

Buller A. L., Larson H. C., Schneider B. E., Beaton J. A., Morrisett R. A., and Monaghan D. T. (1994) The molecular basis of NMDA receptor subtypes: native receptor diversity is predicted by subunit composition. *J. Neurosci.* **14,** 5471–5484.

Buller A. L., Larson H. C., Morrisett R. A., and Monaghan D. T. (1995) Glycine modulates ethanol inhibition of heteromeric *N*-methyl-D-aspartate receptors expressed in *Xenopus* oocytes. *Mol. Pharmacol.* **48,** 717–723.

Choi D. W. (1988) Glutamate neurotoxicity and diseases of the nervous system. *Neuron* **1,** 623–634.

Clements J. D. and Westbrook G. L. (1991) Activation kinetics reveal the number of glutamate and glycine binding sites on the *N*-methyl-D-aspartate receptor. *Neuron* **7,** 605–613.

Daggett L. P., Lu C. C., Crona J., Hess S. D., Johnson E. C., Ellis S. B., and Veliçelebi G. (1994) The human NMDAR2C subunit is struc-

turally and functionally distinct from the rat NMDAR2C. *Soc. Neurosci. Abstr.* **20,** 740.

Deal C., Hess S. D., Washburn M., Veliçelebi G., and Johnson E. C. (1996) Subunit-specific properties of human recombinant NMDA receptors. *Soc. Neurosci. Abstr.* **22,** 590.

Foldes R. L., Adams S. L., Fantaske R. P., and Kamboj R. K. (1994*a*) Human *N*-methyl-D-aspartate receptor modulatory subunit hNR2A: cloning and sequencing of the cDNA and primary structure of the protein. *Biochim. Biophys. Acta* **1223,** 155–159.

Foldes R. L., Rampersad V., and Kamboj R. K. (1994*b*) Cloning and sequence analysis of additional splice variants encoding human *N*-methyl-D-aspartate receptor (hNR1) subunits. *Gene* **147,** 303–304.

Goldin A. L. (1992) Maintenance of *Xenopus laevis* and oocyte injection. *Methods Enzymol.* **207,** 266–279.

Hess S. D., Daggett L. P., Crona J., Deal C., Lu C.-C., Urrutia A., Chavez-Noriega L., Ellis S. B., Johnson E., and Veliçelebi G. (1996) Cloning and functional characterization of human heteromeric *N*-methyl-D-aspartate receptors. *J. Pharmacol. Exp. Ther.* **278,** 808–816.

Hirai H., Kirsch J., Laube B., Betz H., and Kuhse J. (1996) The glycine binding site of the *N*-methyl-D-aspartate receptor subunit NR1: identification of novel determinants of co-agonist potentiation in the extracellular M3–M4 loop region. *Proc. Natl. Acad. Sci. USA* **93,** 6031–6036.

Ho S. N., Hunt H. D., Horton R. M., Pullen J. K., and Pease L. R. (1989) Site-directed mutagenesis by overlap extension using the polymerase chain reaction. *Gene* **77,** 51–59.

Hollmann M. and Heinemann S. (1994) Cloned glutamate receptors. *Annu. Rev. Neurosci.* **17,** 31–108.

Ikeda K., Nagasawa M., Mori H., Araki K., Sakimura K., Watanabe M., Inoue Y., and Mishina M. (1992) Cloning and expression of the ε4 subunit of the NMDA receptor channel. *FEBS Lett.* **313,** 34–38.

Ikeda K., Araki K., Takayama C., Inoue Y., Yagi T., Aizawa S., and Mishina M. (1995) Reduced spontaneous activity of mice defective in the ε4 subunit of the NMDA receptor channel. *Mol. Brain Res.* **33,** 61–71.

Ishii T., Moriyoshi K., Sugihara H., Sakurada K., Kadotani H., Yokoi M., Akazawa C., Shigemoto R., Mizuno N., Masu M., and Nakanishi S. (1993) Molecular characterization of the family of the *N*-methyl-D-aspartate receptor subunits. *J. Biol. Chem.* **268,** 2836–2843.

Karp S. J., Masu M., Eki T., Ozawa K., and Nakanishi S. (1993) Molecular cloning and chromosomal localization of the key subunit of the human *N*-methyl-D-aspartate receptor. *J. Biol. Chem.* **268,** 3728–3733.

Kingston R. E. (1996) Calcium phosphate transfections, in *Current Protocols in Molecular Biology* (Ausubel F. M., Brent R., Kingston R. E., Moore D. D., Seidman J. G., Smith J. A., and Struhl K., eds), pp. 9.1.4–9.1.6. John Wiley & Sons, New York.

Kozak M. (1986) Point mutations define a sequence flanking the AUG initiation codon that modulates translation by eukaryotic ribosomes. *Cell* **44,** 283–292.

Laube B., Hirai H., Sturgess M., Betz H., and Kuhse J. (1997) Molecular determinants of agonist discrimination by NMDA receptor subunits: analysis of the glutamate binding site on the NR2B subunit. *Neuron* **18,** 493–503.

Le Bourdellès B., Wafford K. A., Kemp J. A., Marshall G., Bain C., Wilcox A. S., Sikela J. M., and Whiting P. J. (1994) Cloning, functional coexpression, and pharmacological characterisation of human cDNAs encoding NMDA receptor NR1 and NR2A subunits. *J. Neurochem.* **62,** 2091–2098.

Leff P. and Dougall I. G. (1993) Further concerns over Cheng–Prusoff analysis. *Trends Pharmacol. Sci.* **14,** 110–112.

Liu H., Wang H., Sheng M., Jan L. Y., Jan Y. N., and Basbaum A. I. (1994) Evidence for presynaptic *N*-methyl-D-aspartate autoreceptors in the spinal cord dorsal horn. *Proc. Natl. Acad. Sci. USA* **91,** 8383–8387.

Liu H., Mantyh P. W., and Basbaum A. I. (1997) NMDA-receptor regulation of substance P release from primary afferent nociceptors. *Nature* **386,** 721–724.

Matsui T., Sekiguchi M., Hashimoto A., Tomita U., Nishikawa T., and Wada K. (1995) Functional comparison of D-serine and glycine in rodents: the effect on cloned NMDA receptors and the extracellular concentration. *J. Neurochem.* **65,** 454–458.

Momiyama A., Feldmeyer D., and Cull-Candy S. G. (1996) Identification of a native low-conductance NMDA channel with reduced sensitivity to Mg^{2+} in rat central neurones. *J. Physiol. (Lond.)* **494,** 479–492.

Monyer H., Burnashev N., Laurie D. J., Sakmann B., and Seeburg P. H. (1994) Developmental and regional expression in the rat brain and functional properties of four NMDA receptors. *Neuron* **12,** 529–540.

Mori H. and Mishina M. (1995) Structure and function of the NMDA receptor channel. *Neuropharmacology* **34,** 1219–1237.

Nakanishi S. (1992) Molecular diversity of glutamate receptors and implications for brain function. *Science* **258,** 597–603.

Patneau D. K. and Mayer M. L. (1990) Structure–activity relationships for amino acid transmitter candidates acting at *N*-methyl-D-aspartate and quisqualate receptors. *J. Neurosci.* **10,** 2385–2399.

Planells-Cases R., Sun W., Ferrer-Montiel A. V., and Montal M. (1993) Molecular cloning, functional expression, and pharmacological characterization of an *N*-methyl-D-aspartate receptor subunit from human brain. *Proc. Natl. Acad. Sci. USA* **90,** 5057–5061.

Priestley T., Laughton P., Myers J., Le Bourdellés B., Kerby J., and Whiting P. J. (1995) Pharmacological properties of recombinant human *N*-methyl-D-aspartate receptors comprising NR1a/NR2A and NR1a/NR2B subunit assemblies expressed in permanently transfected mouse fibroblast cells. *Mol. Pharmacol.* **48,** 841–848.

Szatkowski M. and Attwell D. (1994) Triggering and execution of neuronal death in brain ischaemia: two phases of glutamate release by different mechanisms. *Trends Neurosci.* **17,** 359–365.

Tölle T. R., Berthele A., Zieglgänsberger W., Seeburg P. H., and Wisden W. (1993) The differential expression of 16 NMDA and non-NMDA receptor subunits in the rat spinal cord and in periaqueductal gray. *J. Neurosci.* **13,** 5009–5028.

Varney M. A., Jachec C., Deal C., Hess S. D., Daggett L. P., Skvoretz R., Urcan M., Morrison J. H., Moran T., Johnson E. C., and Veliçelebi G. (1996) Stable expression and characterization of recombinant human heteromeric *N*-methyl-D-aspartate receptor subtypes NMDAR1A/2A and NMDAR1A/2B in mammalian cells. *J. Pharmacol. Exp. Ther.* **279,** 367–378.

Wenzel A., Scheurer L., Künzi R., Fritschy J. M., Mohler H., and Benke D. (1995) Distribution of NMDA receptor subunit proteins NR2A, 2B, 2C and 2D in rat brain. *Neuroreport* **7,** 45–48.

Wenzel A., Villa M., Mohler H., and Benke D. (1996) Developmental and regional expression of NMDA receptor subtypes containing the NR2D subunit in rat brain. *J. Neurochem.* **66,** 1240–1248.

Williams K. (1993) Ifenprodil discriminates subtypes of the *N*-methyl-D-aspartate receptor: selectivity and mechanisms at recombinant heteromeric receptors. *Mol. Pharmacol.* **44,** 851–859.

Williams K. (1995) Pharmacological properties of recombinant *N*-methyl-D-aspartate (NMDA) receptors containing the ε4 (NR2D) subunit. *Neurosci. Lett.* **184,** 181–184.

Wo Z. G. and Oswald R. E. (1994) Transmembrane topology of two kainate receptor subunits revealed by *N*-glycosylation. *Proc. Natl. Acad. Sci. USA* **91,** 7154–7158.

Wyllie D. J. A., Béhé P., Nassar M., Schoepfer R., and Colquhoun D. (1996) Single-channel currents from recombinant NMDA NR1a/NR2D receptors expressed in *Xenopus* oocytes. *Proc. R. Soc. Lond. (Biol.)* **263,** 1079–1086.